

Scalar, Tensor and $K^+ \rightarrow \pi^+ X$

Zhe Wang

12 Nov. 2008

Abstract

A note keeps the detail of scalar, tensor and X branching ratio calculation.

Contents

1	Kinematic box cuts of each year	1
2	Resolutions of Kp2 kinematic variables	5
3	Pion spectrum of SM, scalar and tensor	6
4	Scalar and tensor branching ratio	6
5	Partial branching ratio and comparison with phase space acceptance	9
6	$K^+ \rightarrow \pi^+ X$, X is stable	11
7	$K^+ \rightarrow \pi^+ X$, X with finite lifetime	11

1 Kinematic box cuts of each year

This section summarizes the kinematic box cuts used in each analysis.

1.1 E949 pnn2 [1]

E949 pnn2 has two independent kinematic cells. One is ke4 box, the other is out of ke4 box.

Entire box:

$$140 < P < 199 \text{ MeV}/c$$

$$60 < E < 100.5 \text{ MeV}$$

$$12 < R < 28 \text{ cm}$$

Ke4 box (contained by the entire box):

$$165 < P < 197 \text{ MeV}/c$$

$$72 < E < 100 \text{ MeV}$$

$$17 < R < 28 \text{ cm}$$

1.2 E787 pnn2 [2]

Only one box

$$140 < P < 195 \text{ MeV}/c$$

$$60 < E < 95 \text{ MeV}$$

$$12 < R < 27 \text{ cm}$$

1.3 E787 95-97 pnn1 analysis [3]

E787 95-97 pnn1 analysis has two independent kinematic cells. One is the golden region, the other is out of the golden region.

So-called entire box:

$$211 < P < 229 \text{ MeV}/c$$

$$115 < E < 135 \text{ MeV}$$

$$34 < R < 40 \text{ cm}$$

BOX': BOX' only cuts on Kp2 peak side and together with entire box gives the final signal box. It has 4% acceptance loss with respect to the entire box.

$$P_{dev} > 2.625$$

$$E_{dev} > 2.453$$

$$R_{dev} > 2.80$$

Golden box (contained by the entire box):

$$P_{dev} > 2.834$$

$$E_{dev} > 2.673$$

$$R_{dev} > 3.00$$

1.4 E787 98 pnn1 analysis [4, 5]

E787 98 pnn1 analysis has five independent kinematic cells defined by six kp2 and kmu2 tail function.

Upper box: Lower bounds are subject to change according to kp2 background.

$$P < 229 \text{ MeV}/c$$

$$E < 135 \text{ MeV}$$

$$R < 40 \text{ cm}$$

kp2 N=0.00147 (kp2a): They cut on Kp2 peak side. N is the background level and it is used to identify cells in current data file. These kinematic regions have such a relation: $kp2a \supset kp2b \supset kp2c$.

$$P_{dev} > 2.500$$

$$E_{dev} > 2.350$$

$$R_{dev} > 2.700$$

kp2 N=0.00065 (kp2b):

$$P_{dev} > 2.600$$

$$E_{dev} > 2.450$$

$$R_{dev} > 2.800$$

kp2 N=0.00031 (kp2c):

$$P_{dev} > 2.750$$

$$E_{dev} > 2.600$$

$$R_{dev} > 2.950$$

kmu2 tail N=0.013468 (kmu2a): This cuts on Kmu2 peak side. N is the background level. $kmu2a \supset kmu2b \supset kmu2c$

$$p < 229 \text{ MeV}/c$$

kmu2 tail N=0.007405 (kmu2b):

$$p < 228 \text{ MeV}/c$$

kmu2 tail N=0.002975 (kmu2c):

$$p < 227 \text{ MeV}/c$$

1.5 E949 pnn1 [6, 7, 8]

Many conflict is found in the document related to this section. All of E949 pnn1 notes seem not up-to-date. Take Joe's code as the right answer. E949 pnn1 has ten independent kinematic cells defined by eleven kp2 and kmu2 tail function. Seven of them are within 1×1 region.

Upper box: Lower bounds are subject to change according to kp2 background.

$$P < 229 \text{ MeV}/c$$

$$E < 135 \text{ MeV}$$

$$R < 40 \text{ cm}$$

kp2 N=12.414880 (kp2a): They cut on Kp2 peak side. N is the background level. $kp2a \supset kp2b \supset kp2c \supset kp2d \supset kp2e \supset kp2f$

$$Pdev > 2.15$$

$$Edev > 2.15$$

$$Rdev > 2.40$$

kp2 N=6.328350 (kp2b):

$$Pdev > 2.25$$

$$Edev > 2.25$$

$$Rdev > 2.50$$

kp2 N=3.210480 (kp2c):

$$Pdev > 2.35$$

$$Edev > 2.35$$

$$Rdev > 2.60$$

kp2 N=1.306830 (kp2d) 1×1 box:

$$Pdev > 2.50$$

$$Edev > 2.50$$

$$Rdev > 2.75$$

kp2 N=0.740880 (kp2e):

$$Pdev > 2.60$$

$$Edev > 2.60$$

$$Rdev > 2.85$$

kp2 N=0.380730 (kp2f):

$$Pdev > 2.70$$

$$Edev > 2.70$$

$$Rdev > 2.95$$

kp2 N=0.200655 (kp2g):

$$Pdev > 2.80$$

$$Edev > 2.80$$

$$Rdev > 3.05$$

kmu2 tail N=0.005692 (kmu2a): This cuts on Kmu2 peak side. N is the background level. $kmu2a \supset kmu2b \supset kmu2c \supset kmu2d$

$$p < 229 \text{ MeV}/c$$

kmu2 tail N=0.003806 (kmu2b):

$$p < 228 \text{ MeV}/c$$

kmu2 tail N=0.002632 (kmu2c):

$$p < 227 \text{ MeV}/c$$

kmu2 tail N=0.001957 (kmu2d):

$$p < 226 \text{ MeV}/c$$

2 Resolutions of Kp2 kinematic variables

Some box cuts are defined as deviation from kp2 peak. So the resolutions of P/E/R are needed. They are listed in Tab. 1.

Table 1: E787 1998 and E949 2002 P/E/R resolutions [6]

	σ_P (MeV/c)	σ_E (MeV)	σ_R (cm)
E787	2.209	3.205	0.888
E949	2.299	2.976	0.866

2.1 Resolution issue in UMC

With the development of E949 experiment UMC is also upgraded to keep consistent as much as possible with the actual detector performance. However now the up-to-date UMC is going to be used to study the box acceptance of older experiment. This gives a concern whether this will introduce an unexpected systematic error.

With a gaussian smearing the acceptance in a certain range usually decreases. See Tab. 1, the momentum resolution is getting worse and the energy and range

resolutions are better. So one will result in less acceptance and the other two will increase it.

Here only the range of pion track is smeared with a gaussian (mean=0, sigma=0.3) distribution to see the maximum effect. The relative acceptance change is small enough to be negligible. For instance for scalar study in the pnn2 region the relative acceptance change is less than 1%. The systematic uncertainty is far below the sensitivity of this experiment.

3 Pion spectrum of SM, scalar and tensor

Fig. 1 gives momentum distribution of SM, scalar and tensor prediction [9] where they have the same normalization. With respect to SM E787 and E949 experiment has less acceptance to scalar and tensor coupling. The momentum truth and measured momentum, $ptot$, after pnn1 or pnn2 trigger is shown in Fig. 2 and Fig. 3 respectively where they are still normalized to the same number of generated events. The plots with only pnn1 trigger simulation are shown in Fig. 4 and Fig. 5.

4 Scalar and tensor branching ratio

The acceptance of each cell of scalar and tensor model is studied by UMC. Then the acceptance used in SM model branching ratio calculation [1, 10] is scaled according to the ratio between another model and SM. This gives the scalar BR:

$$BR_{scalar} = (9.94^{+8.48}_{-4.20}) \times 10^{-10}$$

$$BR_{scalar} < 20.9 \times 10^{-10} \text{ (90\% C.L.)}$$

For tensor:

$$BR_{tensor} = (4.87^{+3.91}_{-2.43}) \times 10^{-10}$$

$$BR_{tensor} < 10.0 \times 10^{-10} \text{ (90\% C.L.)}$$

The results for some year's analyses and their combinations are tabularized in Tab. 2 and Tab. 3 to help understanding. The analyses done in pnn1 region have very little sensitivity to scalar model due to very limited acceptance.

The result with E787 pnn2 data alone using Junk method is

$$BR_{scalar-this} < 27.0 \times 10^{-10} \text{ (90\% C.L.)}$$

$$BR_{tensor-this} < 17.7 \times 10^{-10} \text{ (90\% C.L.)}$$

which is consistent Bipul's result:

$$BR_{scalar-Bipul} < 27.5 \times 10^{-10} \text{ (90\% C.L.)}$$

$$BR_{tensor-Bipul} < 18.3 \times 10^{-10} \text{ (90\% C.L.)}$$

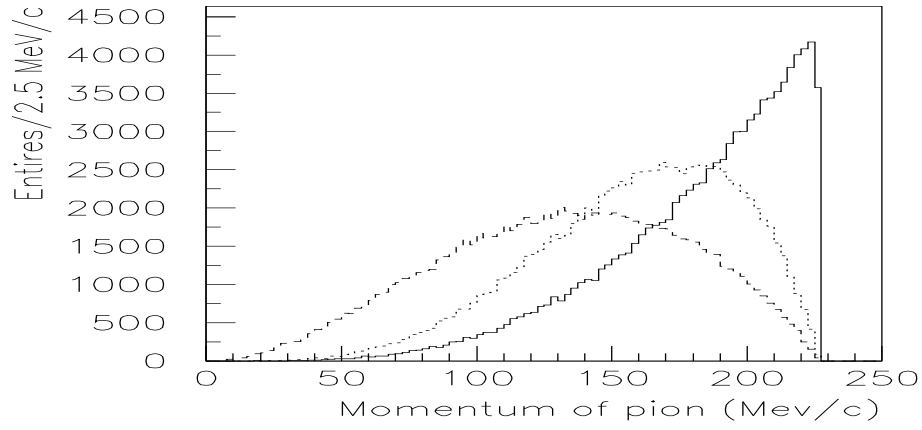


Figure 1: Momentum truth of SM, scalar and tensor prediction. The solid line is for SM, dotted line for tensor and dashed line for scalar. And they have the same normalization.

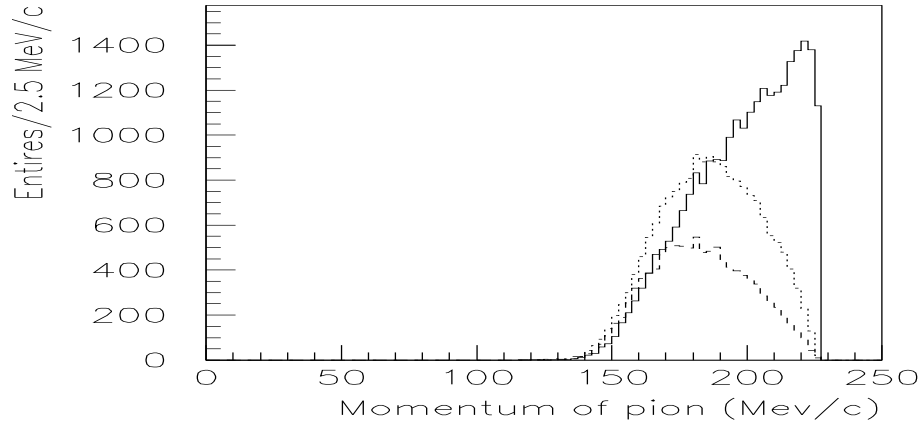


Figure 2: Momentum truth of SM, scalar and tensor prediction after pnn1 or pnn2 trigger simulation. The solid line is for SM, dotted line for tensor and dashed line for scalar where all histogram have been normalized to the same number of generated events.

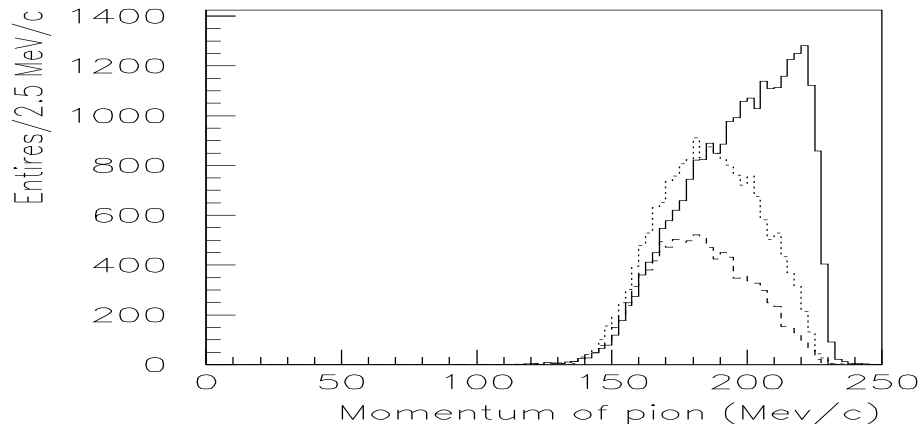


Figure 3: Measured momentum of SM, scalar and tensor prediction after pnn1 or pnn2 trigger simulation. The solid line is for SM, dotted line for tensor and dashed line for scalar where all histogram have been normalized to the same number of generated events.

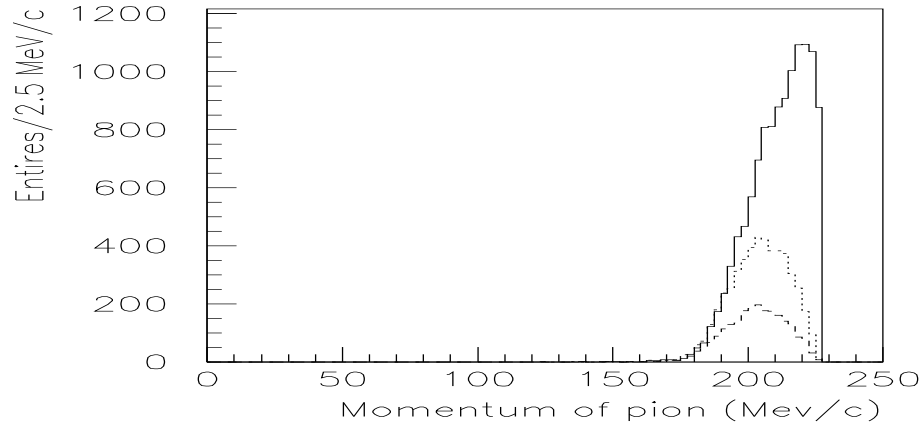


Figure 4: Momentum truth of SM, scalar and tensor prediction after pnn1 trigger simulation. The solid line is for SM, dotted line for tensor and dashed line for scalar where all histogram have been normalized to the same number of generated events.

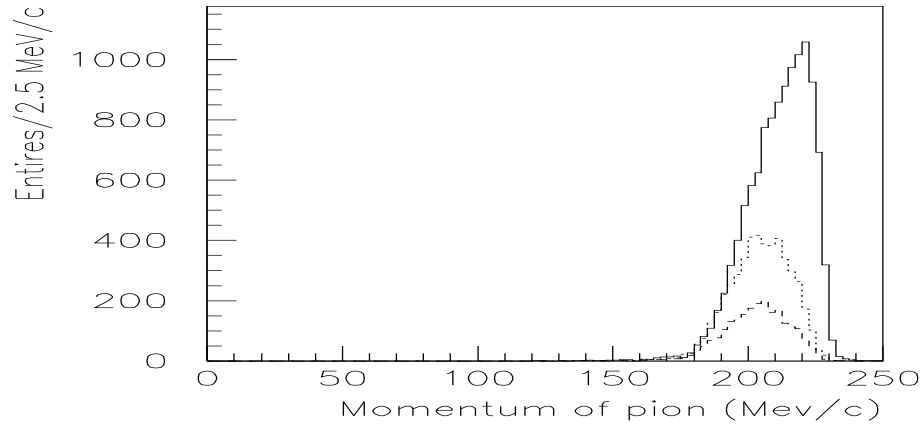


Figure 5: Measured momentum of SM, scalar and tensor prediction after pnn1 trigger simulation. The solid line is for SM, dotted line for tensor and dashed line for scalar where all histogram have been normalized to the same number of generated events.

Table 2: Scalar result from some year's analyses and their combinations

($\times 10^{-10}$)	Branching ration 68%	Upper limit 90%
All E787 and E949	$9.94^{+8.48}_{-4.20}$	20.9
E949 pnn2	$11.6^{+12.7}_{-7.4}$	28.7
98 02 pnn1	$14.8^{+21.4}_{-11.2}$	44.8
9597 pnn1	$14.0^{+33.0}_{-4.6}$	55.9
E787 pnn2	–	27.0
All pnn2	$7.12^{+9.53}_{-4.27}$	19.7
All pnn1	$14.27^{+14.24}_{-8.52}$	33.8

Table 3: Tensor result from some year's analyses and their combinations

($\times 10^{-10}$)	Branching ration 68%	Upper limit 90%
All E787 and E949	$4.87^{+3.91}_{-2.43}$	10.0
E949 pnn2	$7.25^{+8.02}_{-4.70}$	18.1
98 02 pnn1	$5.45^{+8.05}_{-4.14}$	16.8
9597 pnn1	$4.85^{+11.69}_{-1.56}$	19.7
E787 pnn2	–	17.7
All pnn2	$4.53^{+6.18}_{-2.73}$	12.6
All pnn1	$5.11^{+4.66}_{-3.25}$	12.1

5 Partial branching ratio and comparison with phase space acceptance

Using the method and region I and II described in K077 [11] the partial branching ratios of scalar and tensor is calculated. Together with SM prediction they are tabularized in Tab. 4. What's listed along with each branching ratio is the phase space acceptance. A quantity DR, double ratio, is defined as following:

$$DR = \frac{BR_I}{\frac{BR_{II}}{\frac{\epsilon_I}{\epsilon_{II}}}}$$

to test the hypothesis of a model where BR_I and BR_{II} are the partial branching ratios in region I and II respectively, and ϵ_I and ϵ_{II} are the corresponding phase space acceptance. When a hypothesis is true the DR will be close to one.

5.1 Bifurcated gaussian

The error of BR is dominated by statistical error so that during the calculation they are considered as uncorrelated. However the error on each partial is huge, a MC

method is used to calculate the error of DR. A bifurcated gaussian function is used to model every branching ratio.

$$P(x) = \begin{cases} \frac{\sigma_1}{\sigma_1 + \sigma_2} G(\mu, \sigma_1) & x \leq \mu; \\ \frac{\sigma_2}{\sigma_1 + \sigma_2} G(\mu, \sigma_2) & x > \mu. \end{cases}$$

Here $G(\mu, \sigma)$ is a gaussian function with mean μ and standard deviation σ . σ_1 and σ_2 can be understood as positive and negative errors. This is thought to be very close to the real PDF of branching ratio result. Two series of random number, branching ratios, are generated according to this model with the corresponding parameters for each DR calculation. The negative branching ratios are discarded. Then the distribution of DR is got. After normalization that is the PDF of DR. The DR distributions of SM, scalar and tensor are shown in Fig. 6. Due to the low statistic or the big error the most probable and the mean value of DR are not consistent. A central 68% range is found to give the error of DR which is like the error calculation used in branching ratio. All these numbers are summarized in Tab. 4.

Table 4: Partial branching ratio and DR. The unit of BR is $\times 10^{-10}$. DR (no error) result is got by a straightforward calculation without any statistical consideration. DR (mean) result is got by the mentioned MC method using mean as the central value. DR (most probable) result is got by MC method while using most probable value as the central value. DR range (68%) is the central 68% CL range and DR range (90%) is for 90% CL.

	standard model		scalar		tensor	
	BR	ϵ	BR	ϵ	BR	ϵ
Region I	$0.49^{+0.46}_{-0.29}$	33.5%	$0.59^{+0.59}_{-0.35}$	4.14%	$0.49^{+0.45}_{-0.31}$	9.62%
Region II	$2.92^{+4.02}_{-1.79}$	57.1%	$3.49^{+4.69}_{-2.09}$	49.1%	$3.10^{+4.23}_{-1.87}$	68.4%
DR (no error)	0.286		1.999		1.128	
bifurcated gaussian						
DR (mean)	$0.37^{+0.22}_{-0.28}$		$1.73^{+2.61}_{-1.05}$		$1.12^{+1.17}_{-0.77}$	
DR (most probable)	$0.13^{+0.47}_{-0.04}$		$0.92^{+3.42}_{-0.24}$		$0.47^{+1.82}_{-0.12}$	
DR range (68%)	[0.095, 0.59]		[0.68, 4.34]		[0.35, 2.29]	
DR range (90%)	[0.072, 0.82]		[0.49, 5.98]		[0.25, 3.15]	
Cls curve from junk method						
DR range (68%)	[0.082, 0.878]		[0.56, 6.148]		[0.288, 3.324]	
DR range (90%)	[0.036, 2.66]		[0.238, 17.616]		[0.126, 9.552]	

Use which one to say tensor result is favor by our observation? Using mean as center value the result for SM will convey a illusion that DR is 3σ away from 1 when lacking explanation of how error is calculated. Using most probable value as central value scalar is more favored than tensor at the first glance, since the center value of scalar is closer to 1. DR range might be an option.

5.2 CLs curve from junk method

It is also possible to use the CLs curves from junk method to simulate the random distribution of each partial branching ratio. The DR distribution is shown in Fig. 7. The 68% and 90% confidence level range for DR are also listed in Tab. 4.

6 $K^+ \rightarrow \pi^+ X$, X is stable

E787 and E949 experiment is only sensitive to detect π^+ with the momentum range [140,230] (MeV/c) which gives that the relevant mass of X is within [0,260] (MeV/c²), see Fig. 8. Events are simulated at 53 mass points, one point per 5 MeV. 90% C.L. For each point upper limit is calculated with Junk method. With E787 pnn1 and pnn2 result the upper limit and sensitivity are shown in Fig. 9 and Fig. 10 respectively. The combined the result of all E787 and E949 analysis are shown in Fig. 11 and Fig. 12 respectively.

6.1 Disagreement with previous result

When the mass of X is 0, the result can be compared with familon result of previous publication, i.e. 2002 pnn1 paper [12]. They are quite different. The approach used before is described in [2]. The acceptance ratio between X and SM is calculated in a $2\sigma_p$ region, the momentum resolution is 2.2 MeV. When the mass of X is 0, 95A and 98C candidates are excluded from the interested region. This gives a very stringent upper limit. This approach did not stick to the cells predefined in pnn blind analysis. Background is not considered either.

In this analysis the division method before box opening are still in use. The kinematic cells where 95A and 98C are located has very large acceptance for familon. So the relevant upper limit is higher than previous result.

For pnn2 analysis background is high enough and can't be neglected, and there is not a well defined background function due to limited statistic. Those reason stops continuing to use a $2\sigma_p$ region to calculate the upper limit. It makes the pnn1 region result more conservative.

7 $K^+ \rightarrow \pi^+ X$, X with finite lifetime

Here X is assumed to have some finite lifetime and its decay is assumed to be detected and be vetoed 100 percent of the time if it happened within detector. Since $K^+ \rightarrow \pi^+ X$ is a two body decay, π^+ must hit T counter to meet trigger condition, this simplifies the calculation of geometry. T counter is 52 cm long and its inner radius is 45.1 cm. These two parameters define the fiducial region. The outmost detector in barrel part is barrel veto who can cover all the solid angle defined by T counter. The outer radius of BV is 145.3 cm and it is about 1.9 m long. Then the outer surface defines the flying distance at a emission angle, $l(\theta)$.

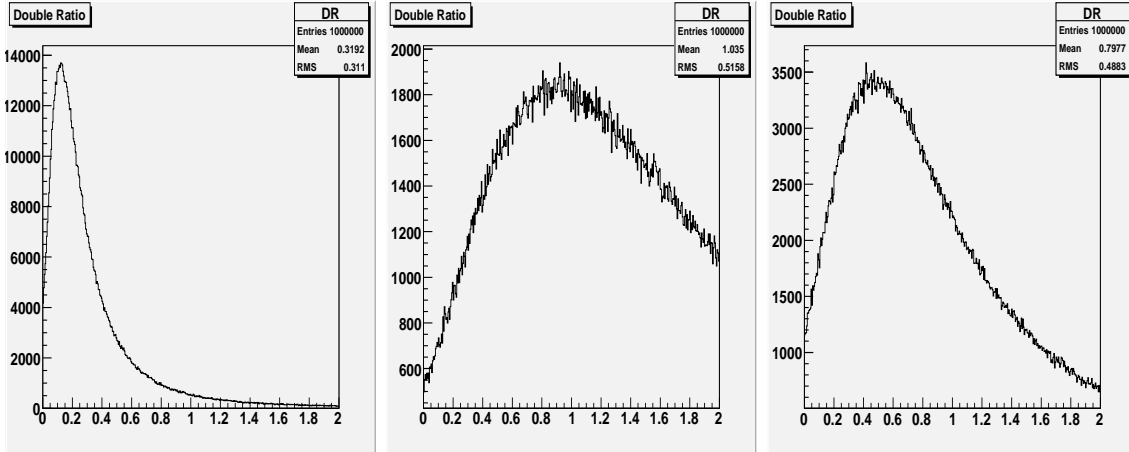


Figure 6: DR distributions from left to right are for SM, scalar and tensor. The partial BR random distribution is simulated by a bifurcated gaussian.

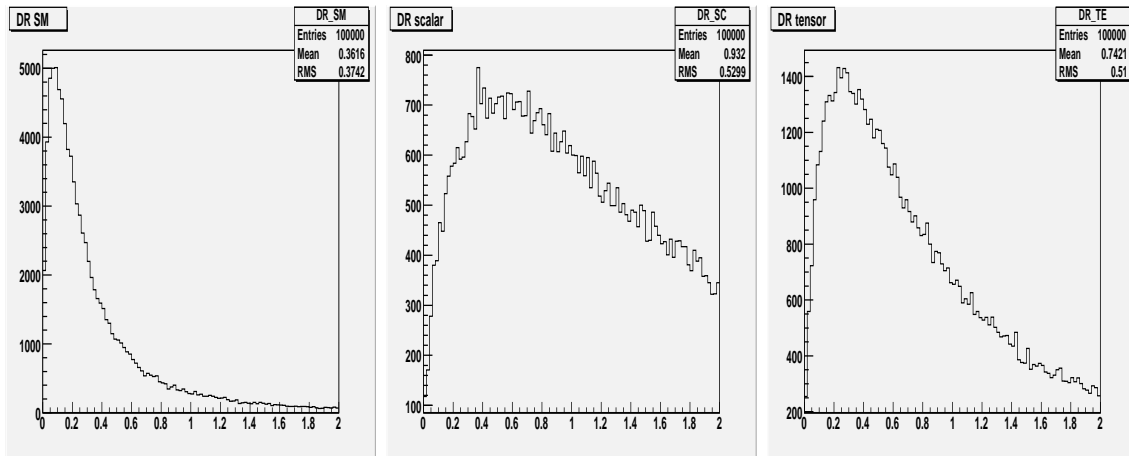


Figure 7: DR distributions from left to right are for SM, scalar and tensor. The partial BR random distribution is simulated by its CLs curve from junk method.

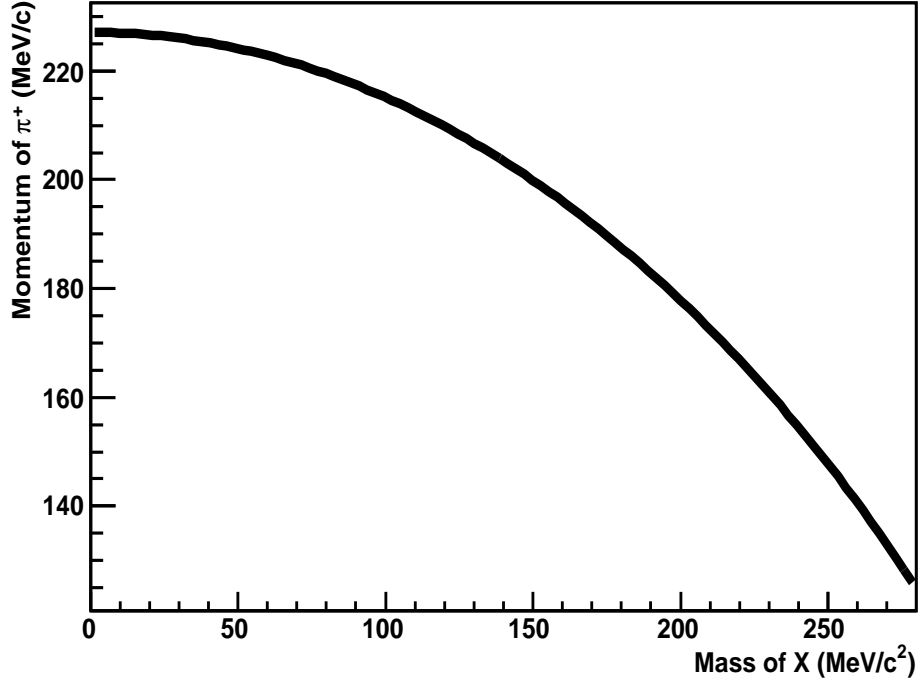


Figure 8: $K^+ \rightarrow \pi^+ X$, π^+ Momentum as a function of the mass of X.

Given the mass, m , and lifetime, τ , of X, the survival probability of X flying out of detector without decay is

$$P_s(m, \tau, \theta) = \exp\left[-\frac{l(\theta)/v(m)}{\tau_l(m, \tau)}\right]$$

where v is the velocity of X, it is a function of m and τ_l is the lifetime of X as a function of m and τ .

The emission direction of X is uniform in space. So the average survival probability is

$$P_{sur}(m, \tau) = \frac{1}{\pi - 2\alpha} \int_{\alpha}^{\pi-\alpha} P_s(m, \tau, \theta) d\theta$$

where α is the boundary defined by T counter.

In last section the BR is calculated as X is stable. If it has a finite lifetime the corresponding BR changes to $BR/P_{sur}(m, \tau)$. The result of lifetime 5 ns, 2 ns, 1 ns, 500 ps, 200 ps and 100 ps is shown in Fig. 13 as well as the case X is stable.

References

- [1] K073
- [2] Bipul's PHD thesis

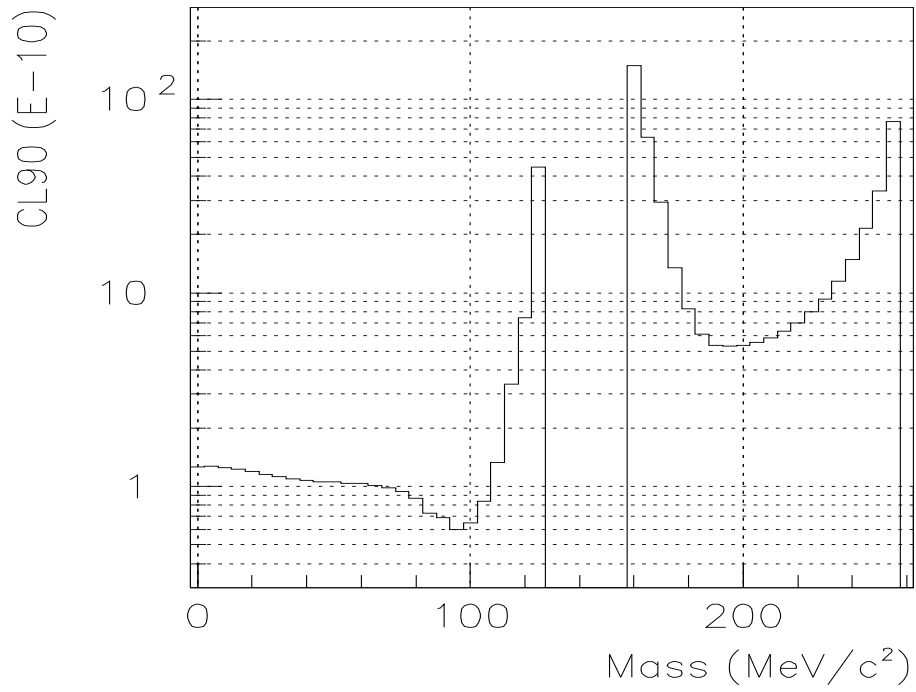


Figure 9: 90% C.L. as a function of the mass of X from E787 result.

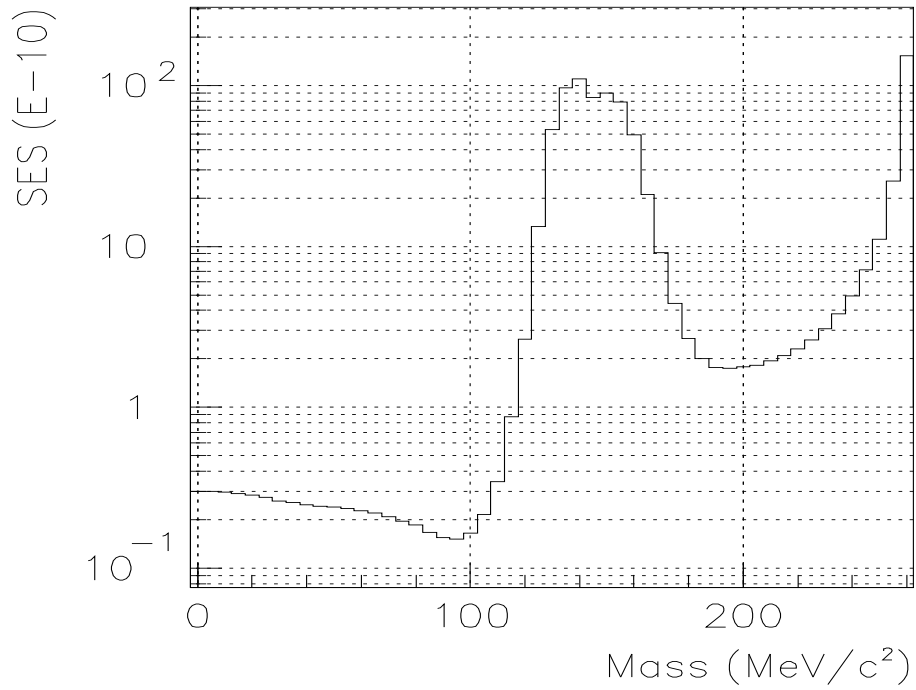


Figure 10: SES as a function of the mass of X from E787 result.

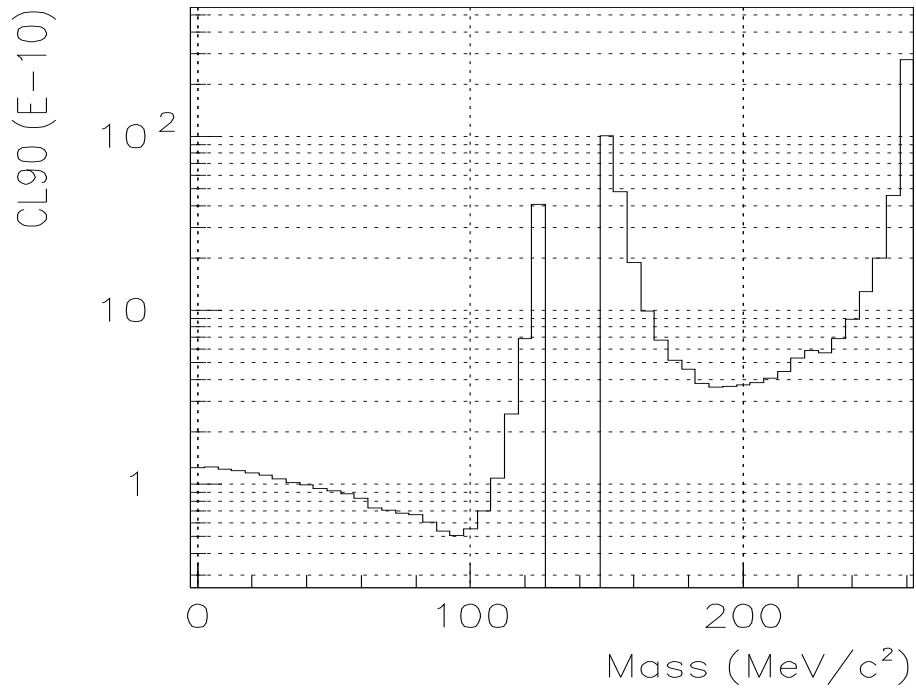


Figure 11: 90% C.L. as a function of the mass of X from all E787 and E949 result.

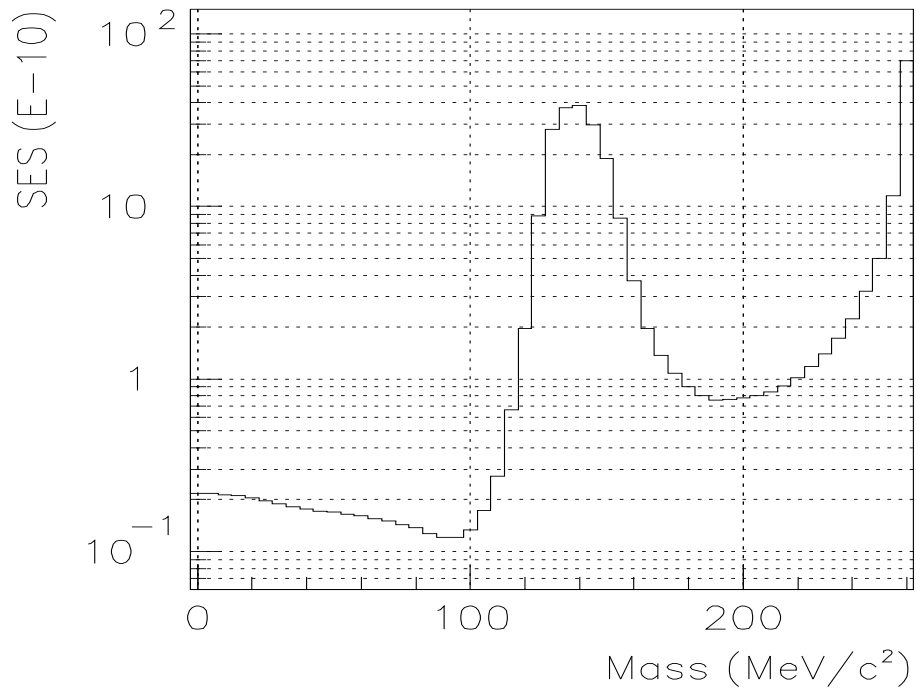


Figure 12: SES as a function of the mass of X from all E787 and E949 result.

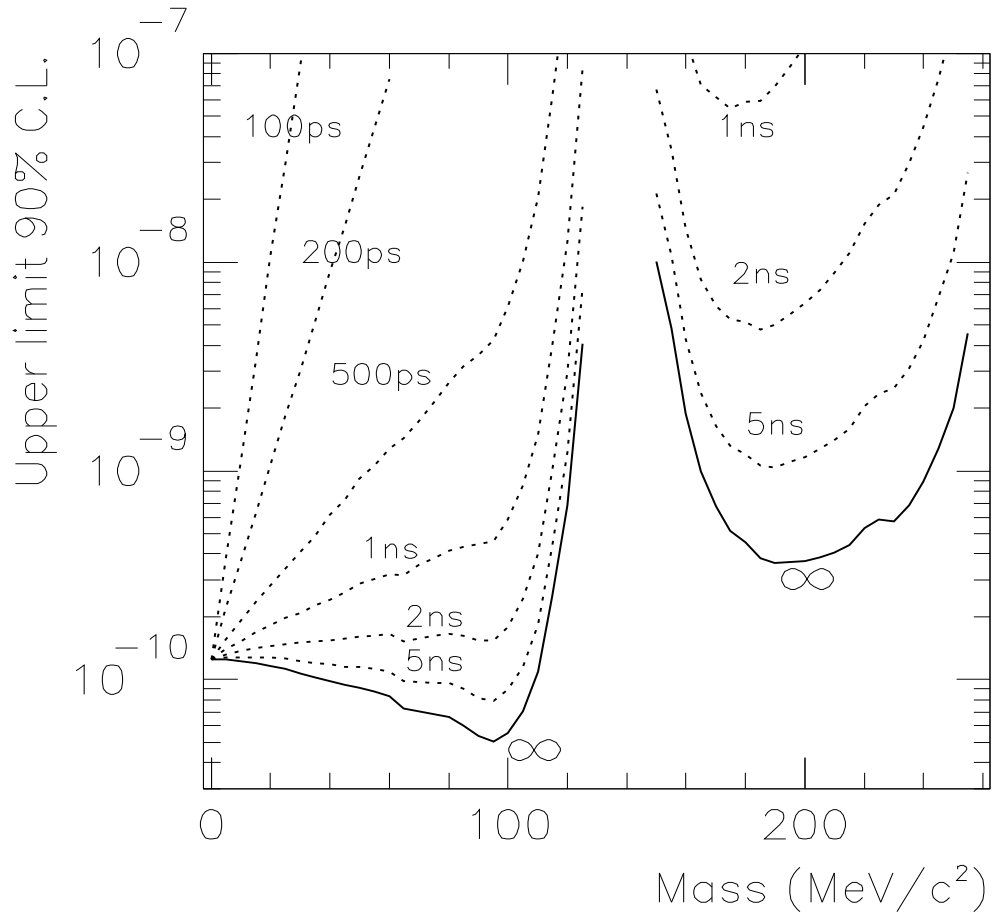


Figure 13: The solid curve gives 90% confidence level upper limit on the branching ratio for $K^+ \rightarrow \pi^+ X$ as a function of the mass of X from all E787 and E949 result where X is stable. The dotted curves give 90% confidence level upper limits for cases where X has a finite lifetime

- [3] tn365
- [4] tn393
- [5] Paul's PHD thesis
- [6] K034
- [7] K038
- [8] Joe's code, bgtotal.c, kp2func.dat, km2tfunc.dat and bgtotal.dat
- [9] Gunnar Kallen, Elementary particle physics, 1964
- [10] K074
- [11] Zhe Wang, E949 technical note K-077 (2008)
- [12] PRL 93, 031801 (2004)